Journal of Power Sources 273 (2015) 561–565

Contents lists available at ScienceDirect

Journal of Power Sources

journal homepage: www.elsevier.com/locate/jpowsour

Short communication

A new lithium-ion battery: CuO nanorod array anode versus spinel $LiNi_{0.5}Mn_{1.5}O_4$ cathode

Weixin Zhang*, Guo Ma, Heyun Gu, Zeheng Yang, He Cheng

School of Chemistry and Chemical Engineering, Hefei University of Technology and Anhui Key Laboratory of Controllable Chemical Reaction & Material Chemical Engineering, Hefei, Anhui 230009, PR China

HIGHLIGHTS

- A full cell is constructed with CuO array anode and spinel $LiNi_{0.5}Mn_{1.5}O_4$ cathode.
- The CuO array is used as binder-free anode without the conventional prelithiation.
- The CuO/LNMO full cell delivers an energy density of 217 Wh kg^{-1} at 0.1C rate.
- The CuO/LNMO full cell exhibits superior rate capability up to 10C rate.
- The CuO/LNMO full cell exhibits good cycle stability.

GRAPHICAL ABSTRACT

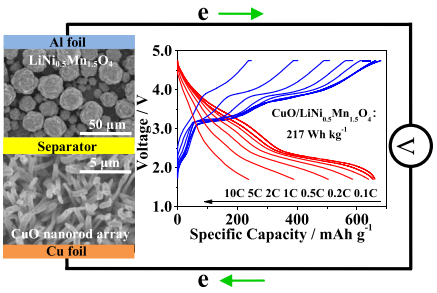

ARTICLE INFO

Article history:
Received 29 July 2014
Received in revised form
19 September 2014
Accepted 20 September 2014
Available online 28 September 2014

Keywords:
Lithium-ion batteries
Copper oxide
Lithium nickel manganese oxides
Nanorod array anode

ABSTRACT

Lithium-ion batteries with advanced performances are required to meet the needs for next generation power batteries. In this work, a new lithium-ion battery has been successfully assembled based on high energy CuO nanorod array anode and high voltage spinel $LiNi_{0.5}Mn_{1.5}O_4$ cathode. Electrochemical tests of the CuO nanorod array grown on copper substrate demonstrate that the CuO/Li half cell can deliver discharge capacities of 787 and 560 mAh g^{-1} at 0.1 and 10C rates. Different from the traditional prelithiation of transition metal oxides anodes, a CuO-limited full cell has been assembled directly by adjusting the positive/negative capacity ratio of 1.2:1, which could deliver a discharge capacity of 660 mAh g^{-1} with estimated energy density of about 217 Wh kg^{-1} at 0.1C rate. The CuO/$LiNi_{0.5}Mn_{1.5}O_4$ full cell exhibits good cycle stability (with capacity retention of 84% at 0.5C over 100 cycles) and superior rate capability (about 240 mAh g^{-1} at a high rate of 10C), which are mainly resulted from CuO arrays directly constructed on copper substrate and the hierarchical structure of $LiNi_{0.5}Mn_{1.5}O_4$ materials. The unique battery may cast new light upon constructing low cost, high energy, high rate capability and high safety full cells.

1. Introduction

Lithium-ion batteries are very promising energy storage system for electric vehicles and portable electronics because of their high energy density and long cycle life [1]. However, current lithium-ion battery technologies are still far from satisfactory to meet the increasingly diverse ranges of applications. To advance battery technologies, it is of great importance to explore novel cathode and anode materials, reasonably match them, and investigate their electrochemical performances [2,3].

Although natural graphite as well as graphitic carbons such as mesocarbon microbeads (MCMB), are the conventional negative electrode materials with capacity of 372 mAh g^{-1} used in lithium-ion batteries, graphite as anode material suffers from several

* Corresponding author. Tel./fax: +86 551 62901450.
E-mail address: wxzhang@hfut.edu.cn (W. Zhang).

http://dx.doi.org/10.1016/j.jpowsour.2014.09.135
0378-7753/

disadvantages in the practical applications [4]. Li-intercalation voltage of graphite is very close to metallic lithium plating and probably leads to the formation of Li dendrites on its surface after repeating cycles, which may result in short circuit and thus bring safety issues especially at high rates. Additionally, graphite has a poor thermodynamic stability during charge–discharge process, which unfavorably affects its cycling stability and rate capacity. Thus, much attention has been paid to alternative and promising anode materials [5–10].

Since the pioneering work done by J.M. Tarascon et al., transition metal oxides (TMOs, M = Co, Ni, Cu, Fe etc.) have aroused much interest as potential anode materials and are expected to achieve further improvements in lithium-ion batteries [5]. In contrast to classical Li^+ insertion and deinsertion process, TMOs as negative-electrode materials can accommodate more lithium ions based on conversion mechanism, thus providing higher specific capacity. Nanosized TMOs are helpful to the reversibility of the conversion reaction.

Among them, copper oxide especially nanosized CuO has been paid much attention because of its high lithium storage capacity (670 mAh g^{-1}) as well as its safe nature (higher voltage plateau) and low cost [6]. However during the lithiation/delithiation conversion process ($CuO + 2Li \leftrightarrow Cu + Li_2O$), the drastic volume variation may cause severe electrode pulverization, which leads to rapid capacity decay and poor cycling stability [7,11,12]. The major drawback limiting the performance and applicability of TMOs electrodes in full cells is its large initial irreversible capacity, which is mainly ascribed to the decomposition of electrolytes and the formation of solid electrolyte interphase (SEI) film due to the catalytic activity of metal nanoparticles produced and the further lithium storage via interfacial charging at the metal/Li_2O interface [7]. To reduce the impact of initial irreversible capacity of TMOs on full cell, some researchers took the strategy of prelithiating in a half cell before full cell assembly [13–15]. For instance, a full cell with Fe_2O_3 powders as anode and $LiFePO_4$ as cathode exhibited a discharge capacity of about 250 mAh g^{-1} (calculated on the mass of the anode) at 0.1C [13]. The Fe_2O_3 anode was prelithiated by discharging against the third lithium electrode. Another full cell employing CuO-MCMB composite anode and $LiNi_{0.5}Mn_{1.5}O_4$ cathode displayed an average capacity of 120 and 112 mAh g^{-1} (calculated on the mass of the cathode) at rates of 0.1C and 5C, respectively [14]. Similarly, the CuO-MCMB anode was electrochemically preactivated by 2 cycles in half cell. Recently, a full cell using the hierarchical MnO powders as anode and $LiNi_{0.5}Mn_{1.5}O_4$ as cathode was reported to have a discharge energy of ca. 350 Wh kg^{-1} at 0.1C [3]. The MnO electrode was also prelithiated by a surface treatment with lithium metal.

Herein, a new lithium-ion battery has been assembled based on CuO nanorod array grown on copper foil as anode and high voltage spinel hierarchical $LiNi_{0.5}Mn_{1.5}O_4$ as cathode. The CuO array film grown on copper foil directly as binder-free anode could allow better electrical contact between the current collector and the active materials, thus leading to a decrease of contact resistance and buffering the large volume changes, which demonstrates good cycle stability and superior rate capability for the TMOs anode based lithium-ion battery. Moreover, different from the prototype pretreatment of lithiation related to TMOs anodes, the full cell can be conveniently assembled just by adjusting the positive/negative capacity ratio, while the lithium ions from the excess cathode can make up the lithium loss during the formation of SEI film on the surface of anode.

2. Experimental

In this work, the CuO nanorod array grown on copper substrate was prepared by a simple liquid–solid reaction under alkaline and oxidative conditions we previously reported [9]. The $LiNi_{0.5}Mn_{1.5}O_4$ (LNMO) material was obtained from BASF SE. The composition and structure of the samples were examined by X-ray diffraction (XRD) on a D/max-γB X-ray diffractometer with a Cu Kα radiation source ($\lambda = 0.154178$ nm) operated at 40 kV and 80 mA. The morphologies of the samples were observed with Hitachi-SU8020 field-emission scanning electron microscope (FESEM) at an accelerating voltage of 5 kV.

The CuO nanorod array on copper substrate was directly employed as binder-free anode. The mass loading of the CuO nanorods on Cu substrate is determined by measuring the mass difference of the CuO electrode before and after removing the copper oxide. The average mass loading of active materials is 1.2 mg and the average loading density of active materials is 0.8 mg cm^{-2} [12]. The LNMO cathode was prepared by mixing 80 wt% active materials, 10 wt% acetylene black and 10 wt% polyvinylidene fluoride and casting slurry onto aluminum foil. The CuO/LNMO full cell was assembled directly, without the conventional prelithiation of the CuO electrode with lithium metal as counter electrode. In order to make up the lithium loss of forming SEI film on the CuO anode surface, the positive/negative capacity ratio was selected to be about 1.2:1 and thus the full cell is an anode-limited cell. The electrolyte was 1 mol L^{-1} $LiPF_6$ in a 1:1 (volume) mixture of ethylene carbonate and dimethyl carbonate, and the separator was a polypropylene membrane with micro-pores (Celgard 2400). The coin-type cells (CR2032) were assembled in an Ar-filled dry glove box. The galvanostatic charge–discharge experiment was conducted using a battery testing system (BTS-5V/10 mA).

3. Results and discussion

Fig. 1a shows the XRD pattern of the as-prepared CuO nanorod array grown on copper substrate, which can be indexed to monoclinic CuO. Fig. 1b and c displays that large scale coverage of CuO nanorods are densely packed on copper substrate with diameters of 300–500 nm and length of 10 μm. Fig. 1d shows the XRD pattern of LNMO materials, in which all of the diffraction peaks correspond to the cubic spinel $LiNi_{0.5}Mn_{1.5}O_4$. The FESEM images in Fig. 1e and f shows that LNMO samples exist in nanoplates-assembled hierarchical microspheres with diameters of 10–25 μm.

The electrochemical performance of both CuO/Li and LNMO/Li half cells was respectively investigated in order to get a thorough understanding of the feasibility of CuO/LNMO full cell. Fig. 2a shows the charge–discharge profiles of the CuO/Li (lower profiles) and LNMO/Li (upper profiles) half cells at various rates. It shows three discharge sloping voltages at about 2.2, 1.4 and 1.0 V, and charge sloping voltage at about 2.1 V. The initial discharge capacity of CuO/Li half cell is found to be 1077 mAh g^{-1}, which is higher than the CuO theoretical capacity of 674 mAh g^{-1}. The corresponding initial coulombic efficiency is about 73%. The CuO/Li still shows a stable discharge capacity of 787 mAh g^{-1} at 0.1C after 5 cycles and even exhibits 560 mAh g^{-1} at 10C, as shown in Fig. 2b. When the current density is decreased from 10C to 0.1C at the end of cycling, the discharge capacity of the CuO/Li can still reach 714 mAh g^{-1}, demonstrating good electrochemical reversibility and structural stability of the CuO nanorod array electrode. As shown in Fig. 2c, the CuO/Li delivers a discharge capacity of 666 mAh g^{-1} with capacity retention of 91% at 0.5C rate after 100 cycles.

In the case of LNMO/Li half cell, three voltage plateaus can be observed from the charge–discharge profiles at around 4.0, 4.65 and 4.75 V as shown in Fig. 2a. As reported, the small plateau at 4.0 V can be associated to the oxidation of Mn^{3+}/Mn^{4+} reaction, and the main 4.65 and 4.75 V plateaus can be associated to the two-step oxidation of Ni^{2+}/Ni^{3+} and Ni^{3+}/Ni^{4+} [16]. From Fig. 2a, the initial discharge capacity is 135 mAh g^{-1}, resulting a coulombic efficiency

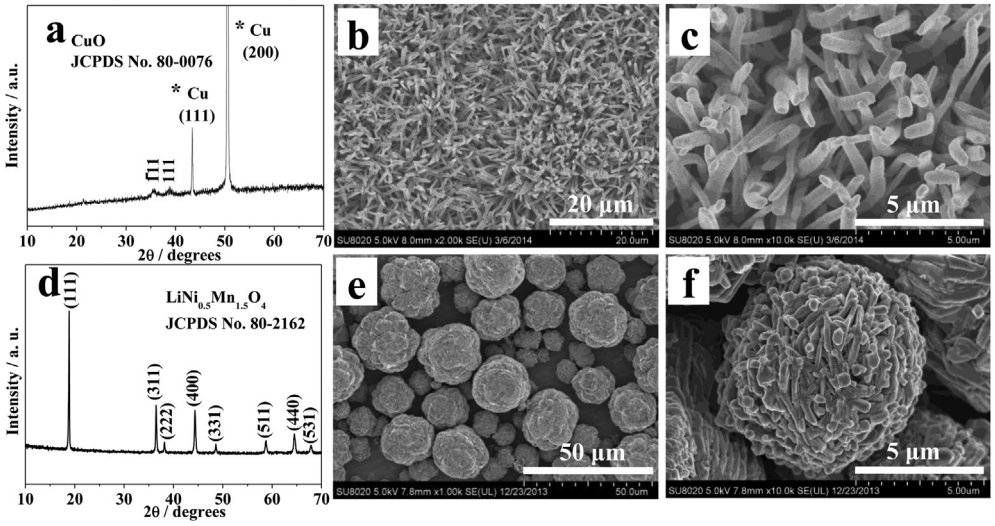

Fig. 1. (a) XRD pattern, (b, c) FESEM images of the CuO nanorod array film anode grown on copper substrate, (d) XRD pattern, (e, f) FESEM images of the LNMO cathode materials.

of 83%. The irreversible capacity is mainly ascribed to the electrolyte decomposition under high voltage [17]. As shown in Fig. 2b, the LNMO/Li can deliver a stable discharge capacity of 135 and 90 mAh g^{-1} after 5 cycles at 0.1C and 10C, respectively. When the current density is decreased from 10C to 0.1C at the end of cycling, the discharge capacity of the LNMO/Li can still reach 134 mAh g^{-1}. Moreover, the LNMO/Li delivers 125 mAh g^{-1} with a capacity retention of 97% at 0.5C rate after 100 cycles (Fig. 2c).

From Fig. 2d, the capacity matchup of the two electrodes can be determined for constructing the CuO-limited full cell. In order to make up the irreversible lithium loss for forming SEI film on the CuO electrode surface, the full cell is assembled directly by controlling the positive/negative capacity ratio of 1.2:1. In the first delithiation of LNMO/Li, the potential of the LNMO/Li remains 4.75 V (point C_1) corresponding to the oxidation of Ni^{3+} to Ni^{4+} at the full cell cutoff voltage of 4.75 V, while CuO/Li drops to 0.005 V (point A_1) in the initial lithiation state for forming a stable SEI film. In the first lithiation of LNMO/Li, the potential of the LNMO/Li drops to 4.65 V (point C_2) corresponding to the reduction of Ni^{3+} to Ni^{2+} and CuO is restored to 2.95 V (point A_2) due to delithiation at the full cell cutoff voltage of 1.70 V. Hence, the voltage range of the CuO-limited full cell is 1.70–4.75 V, and Equation (1) reflects the overall electrochemical process.

$$(x/2)\mathrm{CuO} + \mathrm{LiNi_{0.5}Mn_{1.5}O_4} \underset{\text{Discharge}}{\overset{\text{Charge}}{\rightleftharpoons}} (x/2)\mathrm{Cu} + (x/2)\mathrm{Li_2O} + \mathrm{Li_{1-x}Ni_{0.5}Mn_{1.5}O_4} \quad (1)$$

Fig. 3a shows the charge–discharge profiles of the CuO/LNMO full cell at various rates corresponding to CuO electrode

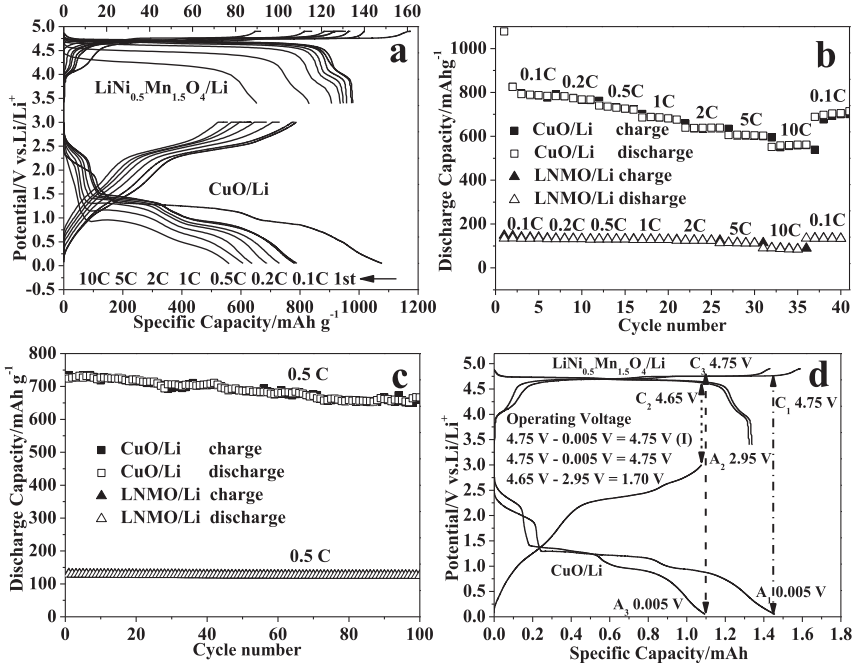

Fig. 2. (a) Charge-discharge profiles, (b) Rate and cycling performance, (c) Cycling performance of the CuO/Li and LNMO/Li half cells, (d) Details of capacity matchup in the CuO-limited full cell.

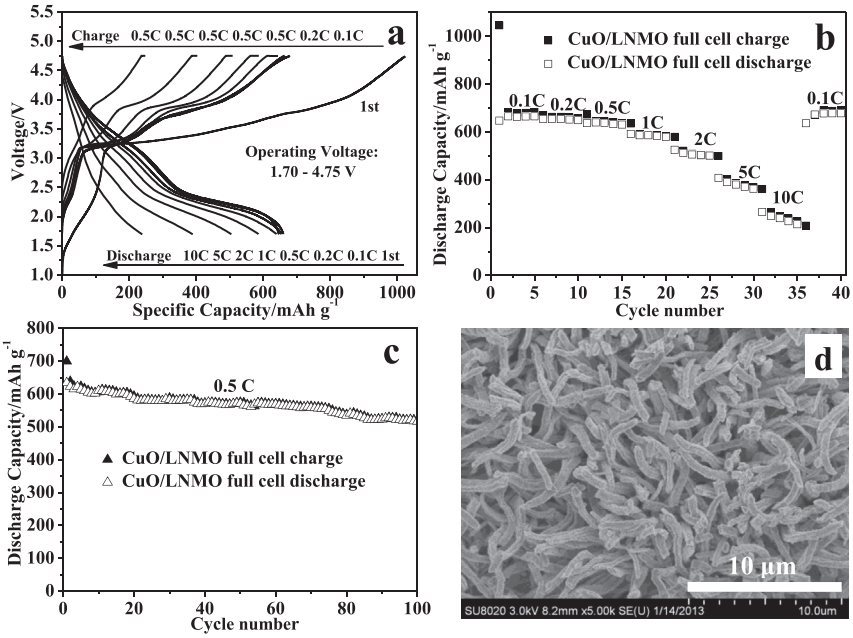

Fig. 3. (a) Charge-discharge profiles, (b) Rate and cycling performance, (c) Cycling performance of the CuO/LNMO full cell, (d) FESEM image of CuO array film anode after 100 cycles of CuO/LNMO full cell at a rate of 0.5C.

(1C = 674 mAh g^{-1}) between 1.70 and 4.75 V versus Li/Li^+. Interestingly, the voltage profiles of CuO/LNMO full cell behave similar to the CuO/Li half cell due to the inherent voltage characteristics of CuO. The full cell can release an initial charge capacity of 1020 mAh g^{-1} and discharge capacity of 650 mAh g^{-1} based on the mass of the CuO electrode at 0.1C with a coulombic efficiency of 64%. As shown in Fig. 3a and b, the CuO/LNMO full cell shows a stable discharge capacity of 660 mAh g^{-1} at 0.1C after 5 cycles and even exhibits 240 mAh g^{-1} at 10C rate, respectively. When the current density is decreased from 10C to 0.1C at the end of cycling, the discharge capacity of the full cell can still reach 677 mAh g^{-1}. Cycling performance of the CuO/LNMO full cell at a rate of 0.5C is shown in Fig. 3c. The CuO/LNMO full cell discharges a capacity of 516 mAh g^{-1} with a capacity retention of 84% at 0.5C rate after 100 cycles.

Here the rate capability of CuO/LNMO full cell is not so consistent with those of CuO/Li and LNMO/Li half cells. It could be ascribed to the following reasons. Firstly, compared with the fixed lithium ions in the full cell, metallic lithium disks as counter electrodes in half cell can provide excess lithium ions, which is beneficial to enhance the electrochemical reaction kinetics of the cells. Secondly, during the continuous charge–discharge processes, undesirable side reactions between lithium and electrolyte could lead to lithium ions loss, especially at high rates [7,17]. For the half cells, metallic lithium disks can provide excess lithium ions to make up this loss, while for CuO/LNMO full cell, the lost lithium ions cannot be compensated. Thirdly, for LNMO/Li half cell, the rate capability decreases during the repeated charge–discharge processes in a mechanism similar to the Mosaic model of $LiFePO_4$/Li system [18]. And for CuO/Li half cell, the rate capability decreases with the conversion reaction ratio decay. However, the rate capability of CuO/LNMO full cell is influenced by both of the conversion reaction ratio of CuO anode and the lithiation/delithiation degree of LNMO cathode, which could not make the CuO/LNMO full cell exhibit accordant rate capability with the CuO/Li and LNMO/Li half cells.

The specific energy (E) of the full cell can be calculated according to Equation (2) [3,19]

$$E = C_{\text{cathode}}C_{\text{anode}}(V_{\text{cathode}} - V_{\text{anode}})/(C_{\text{cathode}} + C_{\text{anode}}) \quad (2)$$

where C indicates the theoretical capacity and V indicates the average potential versus Li/Li^+. The full cell delivers an estimated discharge energy of about 217 Wh kg^{-1} at 0.1C rate.

Structural changes of the electrode material during the charge–discharge process greatly influence its electrochemical properties. Fig. 3d presents the FESEM images of the CuO electrode (in the charged state) after 100 charge–discharge cycles of CuO/LNMO full cell at 0.5C rate. The intact nanorod arrays can still be identified after repeated charge–discharge processes. The results reveal that the CuO array structure is stable, which could buffer the volume changes and improve the rate and cycling performance of the CuO/LNMO full cell.

4. Conclusions

In summary, a new CuO/$LiNi_{0.5}Mn_{1.5}O_4$ full cell with enhanced performances has been successfully assembled based on CuO nanorod array anode and spinel $LiNi_{0.5}Mn_{1.5}O_4$ cathode. Without using conventional pretreatment of the CuO electrode with lithium foil as counter electrode, an anode-limited full cell is assembled simply by controlling the positive/negative capacity ratio of 1.2:1, while the lithium ions from the excess cathode can make up the lithium loss for SEI film on the surface of CuO. It delivers a discharge capacity of 660 mAh g^{-1} at 0.1C rate, with an estimated specific energy density of about 217 Wh kg^{-1}. Moreover, the full cell exhibits a discharge capacity of 240 mAh g^{-1} at a high rate of 10C and capacity retention of 84% at 0.5C over 100 cycles. The excellent superior rate capability and cycle stability of the CuO/$LiNi_{0.5}Mn_{1.5}O_4$ full cell is mainly attributed to well-aligned CuO arrays directly constructed on copper substrate as well as the hierarchical structure of $LiNi_{0.5}Mn_{1.5}O_4$ materials, via enhancing electrical conductivity, and buffering the volume changes during repeated charge–discharge processes. We believe that this work may cast new light upon constructing low cost, high energy, high rate capability and high safety full cells with TMOs as anodes.

Acknowledgments

The authors are grateful to the financial supports of the National Natural Science Foundation of China (NSFC Grants 21176054 and 21271058).

References

[1] A.S. Aricò, P. Bruce, B. Scrosati, J.M. Tarascon, W.V. Schalkwijk, Nat. Mater. 4 (2005) 366–377.
[2] J. Hassoun, K.S. Lee, Y.K. Sun, B. Scrosati, J. Am. Chem. Soc. 133 (2011) 3139–3143.
[3] G.L. Xu, Y.F. Xu, J.C. Fang, F. Fu, H. Sui, L. Huang, S.H. Yang, S.G. Sun, ACS Appl. Mater. Interfaces 5 (2013) 6316–6323.
[4] L.F. Li, B. Xie, H.S. Lee, H. Li, X.Q. Yang, J. McBreen, X.J. Huang, J. Power Sources 189 (2009) 539–542.
[5] P. Poizot, S. Laruelle, S. Grugeon, L. Dupont, J.M. Tarascon, Nature 407 (2000) 496–499.
[6] X.J. Zhang, D.E. Zhang, X.M. Ni, H.G. Zheng, Solid State Electron. 52 (2008) 245–248.
[7] A. Débart, L. Dupont, P. Poizot, J.B. Leriche, J.M. Tarascon, J. Electrochem. Soc. 148 (2001) A1266.
[8] M.B. Wu, J. Liu, M.H. Tan, Z.T. Li, W.T. Wu, Y.P. Li, H.P. Wang, J.T. Zheng, J.S. Qiu, RSC Adv. 4 (2014) 25189–25194.
[9] C.T. Zhao, C. Yu, S.H. Liu, J. Yang, X.M. Fan, J.S. Qiu, Part. Part. Syst. Charact. (2014), http://dx.doi.org/10.1002/ppsc.201400114.
[10] Y. Liu, X.Z. Wang, Y.F. Dong, Z.Y. Wang, Z.B. Zhao, J.S. Qiu, J. Mater. Chem. A (2014), http://dx.doi.org/10.1039/C4TA03531C.
[11] W.X. Zhang, S.H. Yang, Acc. Chem. Res. 42 (2009) 1617–1627.
[12] W.X. Zhang, M. Li, Q. Wang, G.D. Chen, M. Kong, Z.H. Yang, S. Mann, Adv. Funct. Mater. 21 (2011) 3516–3523.
[13] J. Hassoun, F. Croce, I. Hong, B. Scrosati, Electrochem. Commun. 13 (2011) 228–231.
[14] R. Verrelli, J. Hassoun, A. Farkas, T. Jacob, B. Scrosati, J. Mater. Chem. A 1 (2013) 15329–15333.
[15] C. Chae, H. Park, D. Kim, J. Kim, E.-S. Oh, J.K. Lee, J. Power Sources 244 (2013) 214–221.
[16] X.B. Zhu, X.N. Li, Y.C. Zhu, S.S. Jin, Y. Wang, Y.T. Qian, J. Power Sources 261 (2014) 93–100.
[17] J.T. Han, J.B. Goodenough, Chem. Mater. 23 (2011) 3404–3407.
[18] A.S. Andersson, J.O. Thomas, J. Power Sources 97-98 (2001) 498–502.
[19] Y. Yang, M.T. McDowell, A. Jackson, J.J. Cha, S.S. Hong, Y. Cui, Nano Lett. 10 (2010) 1486–1491.